Comparative Analysis of Creep Data for Sn-Ag-Cu Solder Joints in Shear

Jean-Paul Clech

EPSI Inc., P. O. Box 1522, Montclair, NJ 07042, USA

tel: +1 973-746-3796, e-mail: jpclech@aol.com, URL: http://jpclech.com

Abstract

This paper analyzes a small database of isothermal shear creep data for Sn-Ag-Cu (SAC) solder joints of bulk composition close to that of the near-eutectic Sn-3.9Ag-0.6Cu alloy. The data is put in perspective in terms of alloy composition, joint geometry and ageing effects. Conventional hyperbolic sine creep models are developed in an attempt to best capture the effect of temperature and stress conditions on steady-state creep rates for common SAC alloys. While the proposed creep models require further validation, especially at cold temperatures where there is a lack of creep data, it is hoped that the results of this comparative analysis are of use to developers of lead-free solder joint stress/strain analysis and reliability prediction models.

Introduction

The study of shear stress and strain in solder joints of electronic assemblies is of interest for the development of analytical models that describe the shear deformations of solder joints due to the global thermal expansion mismatch between components and circuit boards or other substrates. Given the heightened interest in lead-free electronic assemblies, it is important to develop constitutive models that capture the shear deformations of lead-free solder joints in a reasonably accurate manner.

This paper compares shear creep data from several laboratories with the objective of consolidating compatible datasets under different stress and temperature conditions. Reasons for differences between datasets are also discussed. The study is limited to the analysis of steady-state creep data for common Sn-Ag-Cu (SAC) solder alloys with compositions close to that of the near-eutectic, ternary alloy Sn3.9Ag0.6Cu. Creep rate equations are derived for possible use in lumped parameter stress/strain analysis tools and solder joint life prediction models.

Database Description

The analysis of shear creep data is based on a small database of creep rates and strength data from five independent tests that are referenced in Table 1. The first column in Table 1 gives labels that are used through the remainder of this paper to identify the five datasets. Except for the UC alloy with a 3.0 % Ag content, the composition of the other solders is close to that of the Sn3.9Ag-0.6Cu alloy recommended by the National Electronics Manufacturing Initiative (NEMI) in North America (see: http://www.nemi.org). Process conditions and cooling rates vary across the database. The UC specimens have the unique characteristic that they were aged for four hours at 160 °C after assembly. Such an ageing treatment is expected to reduce the strength of virgin solder joints.

Table 2 summarizes the joint geometry and material information. The geometry is either of the flip-chip type (IZM hour-glass joints) or similar to that of solder joints of Chip Scale Package (CSP) assemblies (NTU specimen) or to more traditional lap-shear joints (NPL, UC and UM specimens). Joint size varies although all designs

Dataset Label	**Reference**	**Alloy Composition**	**Process Conditions**
IZM	Wiese, Schubert et al., 2001	95.5Sn-4.0Ag-0.5Cu	Standard transfer bonding.
NPL	Dušek et al., 2003	95.5Sn-3.8Ag-0.7Cu	Paste reflowed by gas-torch. Water-quenched.
NTU	Pang et al., 2003	95.5Sn-3.8Ag-0.7Cu	250 °C peak reflow.
UC	Morris et al., 2003	96.5Sn-3.0Ag-0.5Cu	N_2 reflow, 235 °C peak, 2.7 °C/sec cooling rate. 4 hour ageing at 160 °C.
UM	Zhang et al., 2003	95.5Sn-3.9Ag-0.6Cu	NA

Table 1: *Sources of shear data, alloy composition (% weight) and process information.*

Dataset	**Joint Geometry / Dimensions**	**Specimen Substrate / Metallization**
IZM	Flip-chip, hour-glass shaped (average stress calculated in mid-height section). 0.15 mm H, 0.1 mm sq. base.	Si chip on Si chip. Cu pads.
NPL	Lap joint. 0.4 mm H x 2 mm L x 2 mm W	Cu fork specimen.
NTU	CSP type, barrel-shaped. 0.32 mm H, 0.4 mm pad Ø , 0.5 mm ball Ø	FR-4 on FR-4 (0.5 mm thick). Cu pads with NiAu finish.
UC	Lap joint. 0.16 mm H × 2.24 mm L × 1.22 mm W	Cu substrate (3.18 mm thick). Cu pad on one side, Ni/Au on other side.
UM	Lap joint. 0.18 mm H × 3 mm L × 1 mm W	Cu substrate (1 mm thick).

Table 2: *Joint geometry, specimen substrate & metallization. H = joint height; L = joint length in the direction of shear; W = width of lap-shear joints. L and W are dimensions of solderable areas.*

attempted to create thin joints with heights similar to those of real solder joints in surface mount assemblies. All specimens had copper pads, either bare or with NiAu plating, or copper substrates. All designs and/or fixturing attempted to minimize specimen bending. This was verified for the NPL specimen (Dušek et al., 2003) using finite element models with an existing constitutive model (Darveaux et al., 1995) for Sn3.5Ag solder.

Stress condition parameters are summarized in Table 3. All tests except for the NTU test were constant-load creep tests. The NTU tests were monotonic strength tests where stress/strain curves are recorded at a given strain rate. In such a case, the maximum shear stress is used as a measure of creep strength. The corresponding creep strength vs. strain rate data generally fits in with creep test data. Strain rates across the five experiments cover a wide range (4×10^{-10} to 10^{-1}/sec). Shear stresses are from 3 to 45 MPa although there are less data points in the lower stress range below 5 MPa. Test temperature is from 5 °C to 130 °C. Our search for SAC data was by no means exhaustive, however, it appears that there is a lack of shear creep data at cold temperatures.

Dataset	Test Type	Temperature	Shear Stress (MPa)	Shear Strain Rate
IZM	Creep	5 °C, 25 °C, 50 °C	13–43	4×10^{-10} to 7×10^{-3}
NPL	Creep	21 °C, 50 °C, 80 °C	10–30	3×10^{-8} to 1×10^{-2}
NTU	Strength (stress/strain)	25 °C, 75 °C, 125 °C	8–35	2.6×10^{-4} to 2.6×10^{-2}
UC	Creep	60 °C, 95 °C, 130 °C	3–15	9×10^{-7} to 2×10^{-2}
UM	Creep	25 °C, 75 °C, 125 °C	4–30	2×10^{-7} to 1×10^{-1}

Table 3: *Isothermal mechanical test conditions, approximate shear stress and strain rate ranges.*

Comparison of Raw Data

General Trends

The raw data is plotted as shear creep rates versus shear stress in Figures 1a-d. The four figures (1a-1d) have the same scales on the horizontal and vertical axis for ease of comparison between datasets. All the data was digitized from figures in the quoted references. The IZM data, which was displayed as tensile data (Figure 19 in Wiese, Schubert et al., 2001) was reconverted to shear using the recommended Von-Mises transformation ($\tau = \sigma/\sqrt{3}$; $\mathring{\gamma} = \mathring{\varepsilon}/\sqrt{3}$ where τ and σ, and $\mathring{\gamma}$ and $\mathring{\varepsilon}$ are shear and tensile stresses and strain rates, respectively). While the applicability of the Von-Mises criterion to SAC solders is not fully established, Pang et al.'s (2003) yield and strength data for bulk specimens in tension and solder joints in shear shows that the Von-Mises stress transformation ($\tau = \sigma/\sqrt{3}$) applies quite well at shear strain rates in the range 2.6×10^{-4} to $2.6\times10^{-2}\text{s}^{-1}$.

All data points are shown in Figure 1a. The database consists of 15 isothermal datasets (3 from each of the five experiments), 53 points for the IZM flip-chip data and 56 points for the other four datasets; that is, a total of 109 data points, 91 of which are at stress levels above 10 MPa. Fifteen data points are in the stress area between 5 and 10 MPa. Only three data points are in the low stress region below 5 MPa, which is the most relevant area for solder joints of electronic assemblies under a variety of use conditions.

Power-law trend lines have been added in Figure 1a to highlight the IZM data and a few other isothermal subsets. This is simply intended to clarify the display of the data without recommending the use of a power-law creep model. Because Figure 1a appears quite busy, the individual datasets are re-plotted two at a time in Figures 1b-d where we have added the slopes, or stress exponents, of the power-law trend lines.

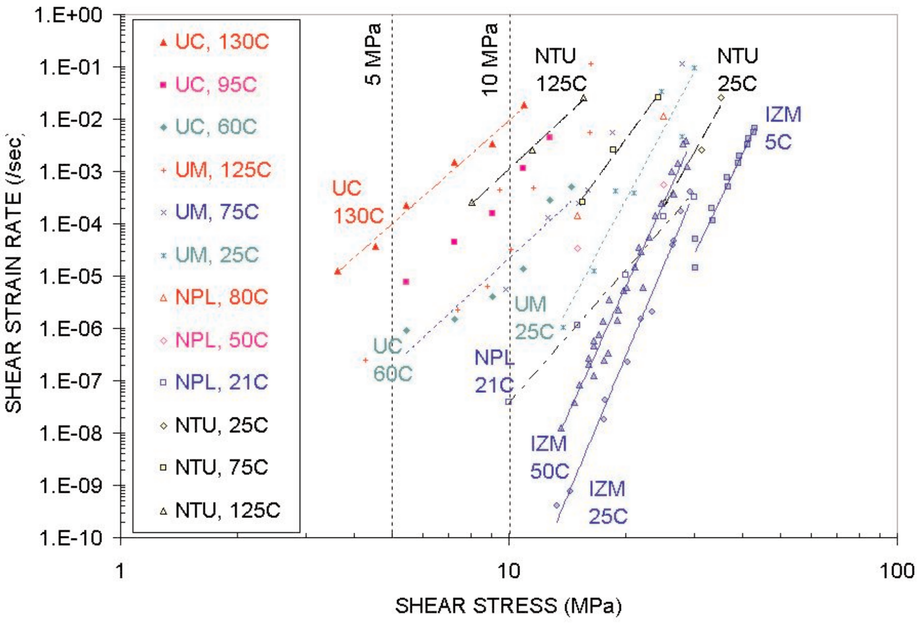

1a: All datasets

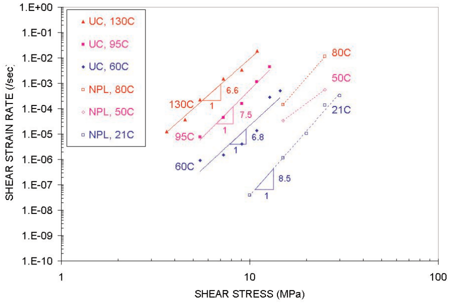

1b: UC and NPL datasets

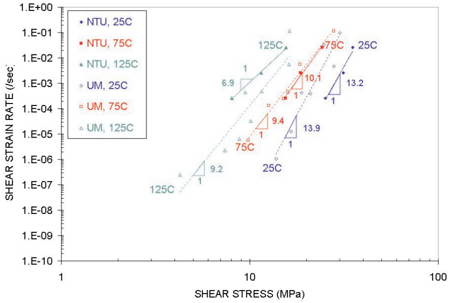

1c: NTU and UM datasets

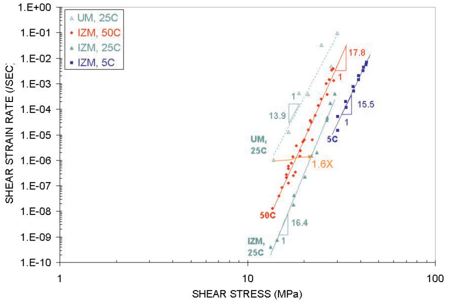

1d: IZM and UM [25 °C] datasets.

Figures 1a-d: *Plots of isothermal steady-state creep data for SAC solder joints in shear.*

From Figures 1a and 1d, the IZM data suggests that the flip-chip joints are more creep resistant than the other joints. In particular, the comparison of the UM and the IZM creep data at 25 °C (Figure 1d) indicates that the IZM flip-chip joints are about 1.6 times stronger than the UM lap-shear joints. Given the high-values of the power-law stress exponents (13.9 to 17.8 in Figure 1d), such a difference in creep strength translates into differences of over two orders of magnitude in steady-state strain rates. It is not clear to this author why that is, although one possible reason is that the small size flip-chip joints cooled much faster than the lap-shear joints in the UM experiment. Faster cooling yields a finer microstructure that is in general more creep resistant. From the joint dimensions in Table 2, the volume of the UM lap-shear joints is roughly 700 times larger than that of the IZM flip-chip joints. Even if the actual cooling rates (in °C/sec) were the same, and because of volume differences, the smaller flip-chip joints cool much faster than the larger UM joints. These effects are still the subject of investigations and cannot be addressed until quantitative measurements of micro-structural features become available.

A cursory look at the trend lines in Figures 1b-d suggests a power-law breakdown with lesser slopes (6.6 to 9.4) in the low to medium stress region to the left, and greater slopes (10.1 to 17.8) in the high stress region to the right. This is indicative of different creep mechanisms being dominant in those two regions. To this author's knowledge, the hard metallurgical evidence for detailed creep mechanisms in SAC solders is not available yet. Thus, for practical purposes, and until fundamental metallurgical studies are completed, the creep test results are best exploited by fitting the data to conventional creep models.

Shear Creep Data at 21-25 °C, 75-80 °C and 125-130 °C

Figures 2a-c are plots of creep data in the small temperature ranges 21 to 25 °C (= 294 to 298 °K), 75 to 80 °C (= 348 to 353 °K) and 125-130 °C (398 to 403 °K), respectively. On the absolute scale (degree Kelvin), the minimum and maximum temperatures of those temperature ranges are within 1.5 % of each other. It is thus legitimate to merge compatible datasets within each of those temperature ranges.

Figure 2a shows that, to a first order, the UM (25 °C), NPL (21 °C) and NTU (25 °C) data fit together rather well. Similar conclusions hold with an even better fit for the UM (75 °C), NPL (80 °C) and NTU (75 °C) data in Figure 2b, and for the UM(125 °C) and NTU(125 °C) data in Figure 2c. The NTU joints are rather small and are representative of chip scale package assemblies, whereas the NPL and UM joints are lap-shear joints of longer dimensions in the direction of shear. Thus, in the three temperature ranges of interest, the steady-state shear creep data from the three experiments fit together, regardless of joint size. The results from the UM, NPL and NTU experiments are consistent with each other and can legitimately be merged in the development of creep models. Note also that, since the creep data derived from the NTU strength test fits rather well with the UM and NPL creep test results, the more rapid strength test may be a viable solution for data acquisition at low strain rates. Last, as expected, small variations in alloy compositions (95.5Sn-3.9Ag-0.6Cu for the UM joints, 95.5Sn-3.8Ag-0.7Cu for the NPL and NTU specimens) do not result in any noticable effect on steady-state creep rates.

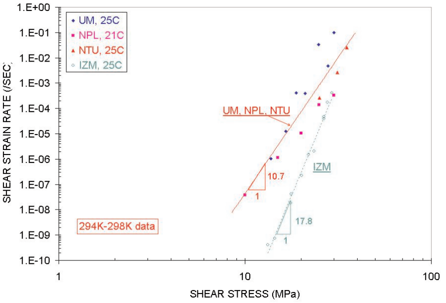

2a: Shear creep data at 21-25 °C.

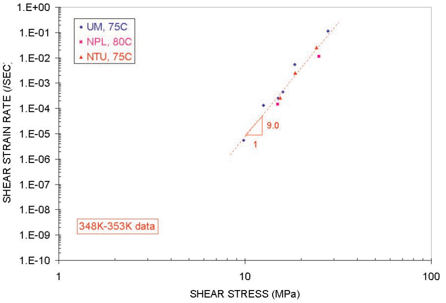

2b: Shear creep data at 75-80 °C.

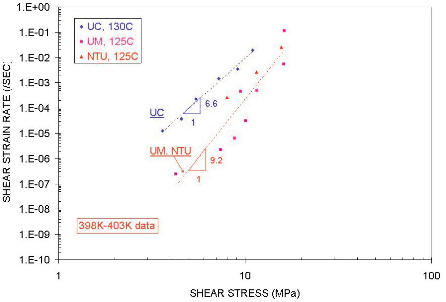

2c: Shear creep data at 125-130 °C.

Figures 2a-c: *SAC steady-state shear creep data in temperature ranges: 21-25 °C, 75-80 °C and 125-130 °C.*

As previously discussed, Figure 2a also shows that the IZM flip-chip joints are more creep resistant and follow a different trend than the UM, NPL and NTU joints. Also, in Figure 2c, the UC (130 °C) data lies above the UM (125 °C) and NTU (125 °C) data by about one to two orders of magnitude along the strain rate axis. Since the temperatures, 125 °C and 130 °C are within 1.3 % of each other on the absolute scale, temperature alone does not explain the large separation between the UC and UM/NTU datasets. The UC solder, Sn3.0Ag0.5Cu, has a somewhat lower content of alloying elements than the UM and NTU solders, Sn3.9Ag0.6Cu and Sn3.8Ag0.7Cu, respectively. However, from a previous study of tensile properties of SAC alloys (Clech, 2003), the three compositions should give rather similar creep rates, at least to a first order. The remaining differentiating factor of the UC joints is the 4 hour ageing at 160 °C after specimen assembly. Annealing is intended to soften metals and this seems to hold for SAC solders as well. For example, the tensile strength of SAC specimens at room temperature was found to decrease by 30 % following five hours of ageing at 125 °C (Fouassier, 2001).

Creep Model Parameters

As a first attempt to consolidate the shear creep data, the creep test results are fitted to a classical hyperbolic sine ("sinh") model:

$$\overset{\circ}{\gamma}\,(/\mathrm{sec}) = A\cdot\left[\sinh(B\cdot\tau\,(MPa))\right]^{n}\cdot\exp\left(-\frac{Q\,(J/mole)}{RT\,(^{\circ}K)}\right) \quad (1)$$

where the steady-state shear strain rate $\overset{\circ}{\gamma}$ (/second) is a function of stress τ (MPa) and absolute temperature T (°K). R =8.314 J/(°K·mole) is the universal gas constant. The four parameters: A, B, n, and the activation energy Q are obtained by regression of the data using the non-linear, multiple variable curve-fitting program "Datafit" by Oakdale Engineering. The hyperbolic sine model has been found to work well for several solder alloys including SnPb and Sn3.5Ag solders (Darveaux et al., 1995). The model reduces to a power law in the low stress area ($B\cdot\tau < 0.8$) and to an exponential model in the high stress area ($B\cdot\tau > 1.2$). Because of the wide range of strain rates, the analysis was conducted on $Y=\ln(\overset{\circ}{\gamma}(/\mathrm{sec}))$ and the regression function was specified as:

$$Y = \ln(\overset{\circ}{\gamma}) = LNA - \frac{Q_a}{T\,(K)} + n\cdot\ln\left[\sinh(B\cdot\tau\,(MPa))\right] \quad (2)$$

where T(°K) and τ (MPa) are independent variables and the regression constants LNA and Q_a are defined as LNA = ln(A) and $Q_a = Q/R$. The regression constants are given in Table 4 with central values followed by standard errors after the ± symbol or minimum and maximum values (central values ± one standard error).

Isothermal lines for each individual model and the corresponding data points for each of the five experiments are plotted in Figures 3a-e. As expected, each model fits the corresponding data quite well. However, the shape of the various models varies, reflecting the range of values of the model parameters in Table 4. For the four datasets other than IZM, the central values of the exponent n vary from 4.31 to 7.94. If we con-

Dataset	**A (/sec) Central Value**	**LNA = ln[A(/sec)]**	**B (MPa^{-1})**	**n Central (min, max)**	**$Q_a = Q/R$ (K)**	**Q Central (min, max) (kJ/mole)**
IZM	1.29×10^{29}	67.028 ±147.08	0.0037 ±0.0321	16.82 (15.9, 17.7)	11388 ±624	94.7 (89.5, 99.9)
NPL	1.70×10^{4}	32.767 ±134.74	0.0773 ±0.126	8.03 (6.10, 9.96)	8547 ±773	71.1 (64.6, 77.5)
NTU	1.52×10^{9}	21.145 ±2.166	0.0895 ±0.0206	5.13 (3.28, 6.97)	11210 ±735	93.2 (87.1, 99.3)
UC	6.47×10^{8}	20.288 ±3.105	0.1739 ±0.0810	4.31 (2.97, 5.65)	11884 ±624	98.8 (93.1, 104.5)
UM	2.82×10^{5}	12.550 ±5.542	0.0624 ±0.0267	7.94 (6.38, 9.50)	7351 ±1170	61.1 (51.4, 70.8)
UM (after Zhang et al., 2003)	248.4	NA	0.188 NA	3.7884 NA	7567 NA	62.9 NA
NPL + NTU + UM (merged data)	1.89×10^{10}	23.644 ±9.284	0.0302 ±0.0255	8.67 (7.36, 9.97)	8772 ±920	72.9 (65.2, 80.6)

Table 4: "Sinh" model regression constants and standard errors or minimum and maximum values (NA = Not Available).

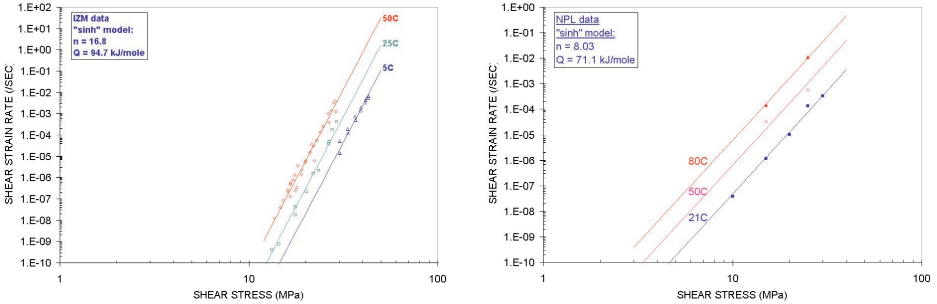

3a: IZM data and "sinh" model isothermal lines.

3b: NPL data and "sinh" model isothermal lines.

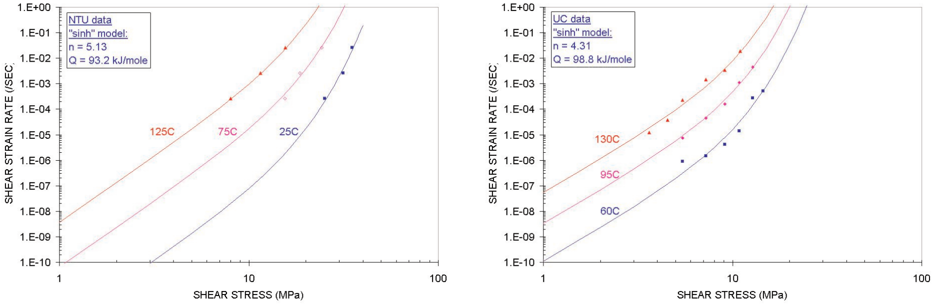

3c: NTU data and "sinh" model isothermal lines.

3d: UC data and "sinh" model isothermal lines.

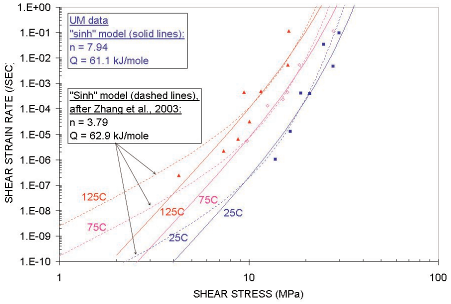

3e: UM data and "sinh" model isothermal lines.

Figures 3a-e: *Fit of hyperbolic sine ("sinh") models to individual datasets of SAC shear creep data. Model parameters for each separate dataset and model are as given in Table 4. Central values of "stress" exponents (n) and activation energies (Q) are also shown on each figure.*

sider the minimum and maximum values that account for standard deviations, n values range from 2.97 to 9.50. Central values of the activation energy Q for the five datasets vary from 61.1 to 98.8 kJ/mole. Accounting for the minima and maxima, Q covers the range 51.4 to 104.5 kJ/mole. One reason for these wide variations in model parameters is the fact that each dataset only covers a limited range of stresses, strain rates or temperatures. This also suggests that any model derived from a single dataset does not necessarily apply across the board and needs to be validated against independent data.

Data points and the corresponding isothermal lines of the "sinh" model for the merged datasets (NPL+NTU+UM) are plotted in Figures 4a-b. Each solid line is based on central values of the

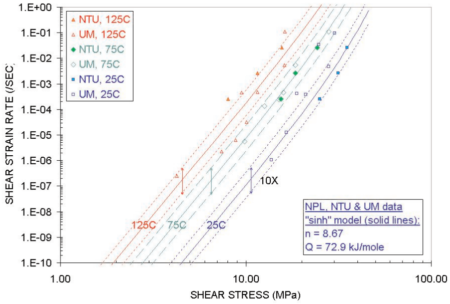

4a: NTU & UM data, and "sinh" model (merged data).

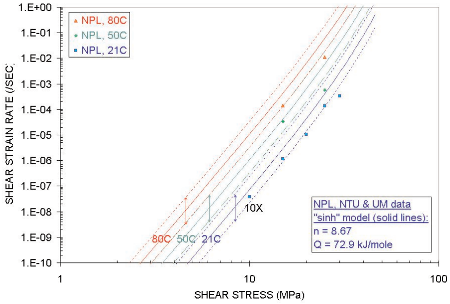

4b: NPL data and "sinh" model (merged data).

Figures 4a-b: *Fit of hyperbolic sine ("sinh") model to SAC shear creep data from NPL + NTU + UM experiments (merged datasets). Central values of "stress" exponent" (n) and activation energy (Q) from last row in Table 4 are also shown.*

"sinh" model parameters. For each temperature of interest, the dashed lines in Figures 4a-b represent lower and upper bounds that are defined by an arbitrary factor √10 ≈ 3.16 times below or above the solid lines. These lower and upper bounds define a "10X" correlation band around the model centerlines. At a given temperature, most data points from the merged datasets fall within or close to the corresponding correlation band. While Figures 4a-b show some scatter, the merged dataset model has the advantage of covering a wider range of stresses and strain rates than the other models that are fitted to a single dataset.

In the present analysis, the "sinh" model for the UM dataset gives different values of the model parameters than those reported by Zhang et al. (2003). While the activation energies are very close (61.1 versus 62.9 kJ/mole), the n exponents are quite different: 7.94 versus 3.79. The original UM data and isothermal lines for the two "sinh" models are plotted in Figure 3e showing that both models fit the data equally well in the experimental range of stresses and strain rates. However, the two models diverge in the area of low stresses or low strain rates. It is not clear to this author why the two models, especially the n exponent values, are so different. The publication by Zhang et al. (2003) does not provide details about the curve-fitting tool or procedure that was used to fit the experimental data.

Last, the exponent n for the IZM dataset (n=16.8) is much larger than the others. Since B·τ << 1 for the experimental stress range in the IZM experiment, the "sinh" model reduces to a power-law creep model and the exponent n=16.8 (15.9 min., 17.7 max.) of the "sinh" model is very close to the power-law exponent of 18 given by Wiese, Schubert et al. (2001).

Comparison of Sn-Ag-Cu and Sn-3.5Ag in Shear

Values of creep parameters from the above analysis of SAC creep data and from a previous analysis of Sn-3.5Ag creep data in shear (Clech, 2003) are summarized in Table 5:

- The first two rows in Table 5 give model parameters for merged datasets of mostly lap-shear creep data. The overlapping values of creep model parameters suggest that similar creep mechanisms are at work for these SAC and Sn-3.5Ag solder joints.
  - The activation energies for SAC and Sn-3.5Ag are in the same narrow range (72.9 to 77.4 kJ/mole for the central values) and the ranges of minimum and maximum Q values overlap.

ALLOY	Number of datasets & specimen type	Reference of data analysis	Q (min, max) kJ/mole	n (min, max)
SAC	3 datasets: NPL + NTU + UM (lap shear & CSP joint)	Present study	72.9 (65.2, 80.6)	8.67 (7.36, 9.97)
Sn-3.5Ag	7 datasets: lap shear and plug & ring joints	Clech, 2003	77.4 (67.5, 87.2)	8.67 (7.58, 9.76)
SAC	1 dataset (NTU): CSP joint type, FR-4 on FR-4 (from Pang et al., 2003)	Present study	93.2 (87.1, 99.3)	5.13 (3.28, 6.97)
Sn-3.5Ag	1 dataset: chip-carrier joints, ceramic on ceramic (from Darveaux et al., 1995)	Clech, 2003	74.5 (71.3, 77.6)	5.54 (5.27, 5.82)

Table 5: *Steady-state creep parameters for SAC and Sn-3.5Ag solder joints in shear: central values of activation energy Q and "sinh" model exponent n. Minimum and maximum values in parenthesis are obtained from standard deviations given by the "Datafit" regression software.*

  - The central values of the n exponents are exactly the same (n=8.67) and the ranges of minimum and maximum values for n overlap as well.

- The last two rows in Table 5 give model parameters for individual datasets of shear data acquired on CSP or ceramic chip carrier solder joints.
  - Contrary to the SAC vs. Sn-3.5Ag merged datasets discussed above, the activation energies for the two solder alloys are quite different: 93.2 kJ/mole for SAC versus 74.5 kJ/mole for Sn-3.5Ag. The latter value is in the range of activation energies for the merged datasets above (72.9 to 77.4 kJ/mole).
  - The "sinh" stress exponents for the two datasets are very close: 5.13 for SAC versus 5.54 for Sn-3.5Ag, however, they are 56 % to 69 % less than the exponent n=8.67 for the merged datasets discussed above.

The general trend is consistency of the "sinh" model parameters for merged datasets of SAC or Sn-3.5Ag shear data. However, it appears that stress exponents are less for individual datasets based on shear testing of joints that closely mimic solder joints of electronic assemblies.

Comparison of Shear and Tensile Model Parameters

"Sinh" model creep parameters for SAC and Sn-3.5Ag in tension (bulk specimens) are summarized in Table 6. The activation energy Q and exponent n values from the various analysis of tensile data are rather consistent. In particular, the results based on SAC data (merged datasets from three independent experiments) and Sn-3.Ag-1.0Cu data (1 experiment) are very similar.

However, the SAC activation energies derived from the analysis of tensile data (Q ~ 59 kJ/mole) are 22 % to 58 % lower than activation energies obtained from the analysis of shear creep data (Q~72 to 93 kJ/mole in Table 5). These differ-

ALLOY	Number of datasets in analysis	Reference data analysis	Q (min, max) kJ/mole	n (min, max)
SAC	3 datasets	Clech, 2003	59.0 (50.9, 67.1)	4.96 (4.20, 5.72)
Sn-3.5Ag-1.0Cu	1 dataset	Atsumi, 2000	59.1	4.9
Sn-3.5Ag	5 datasets	Clech, 2003	57.0 (48.4, 65.5)	4.89 (4.31, 5.47)
Sn-3.5Ag	1 dataset	Atsumi, 2000	50.3	3.6

Table 6: *Steady-state tensile creep parameters for SAC and Sn-3.5Ag solders: central values of activation energy Q and "sinh" model exponent n. Minimum and maximum values in parenthesis are obtained from standard deviations given by the "Datafit" regression software.*

ences, which are not understood, are essentially based on the use of the Arrhenius factor to capture the temperature dependence of creep rates and are independent of the choice of the stress function ("sinh" factor in equation (1)).

The SAC exponent n in tension (n ~ 4.9-5.0 in Table 6) is also different from the SAC exponent for lap-shear joints and the merged SAC datasets in Table 5 (n = 8.67). However, the n exponent of about 5 in tension is consistent with exponents of 5.13 and 5.14 in Table 5 for CSP and chip carrier solder joints in shear.

Conclusions

A review and comparative analysis of SAC shear creep data was conducted. The review is not exhaustive and will need to be updated when additional data becomes available. Although limited in scope, our search for shear creep data indicates a scarcity of or an apparent lack of data:

- At temperatures below 5-21 °C.
- At stress levels below 5 MPa.

Some scatter in the data was observed although trends are clearly visible. Of the five datasets that were studied:

- Three appeared to fit well together. Their alloy composition was in the narrow range: Sn-3.8Ag-0.7Cu, Sn3.9Ag0.6Cu and the joint geometries were of the lap-shear or CSP joint type.
- One dataset appeared to be less creep resistant than the others. While its composition was slightly different (Sn-3.0Ag-0.5Cu), our previous analysis of tensile creep data (Clech, 2003) has shown that the reduced Ag contents – 3.0 % vs. 3.8-3.9 % for the other datasets – is not large enough to explain the loss of creep strength. We believe that the 4 hour ageing of test specimens at 160 °C was a more significant factor contributing to the reduction in creep resistance.
- The last dataset (flip-chip joints) clearly showed higher creep resistance than all the others. The same dataset displayed a very high stress exponent in power-law or "sinh" creep models. This is perhaps indicative of a minimum or threshold stress below which dislocation motions are blocked due to dispersed precipitates in the SAC solder. Such a behavior has been observed in the analysis of Sn-0.7Cu tensile data and a threshold-stress creep model was proposed to describe the steady-state creep data (Wu et al., 2002).

The hyperbolic sine creep model was found to fit the shear creep data reasonably well, at least within the experimental range:

- Several models were suggested with parameters given in Table 4, depending on which dataset is analyzed. Which set of parameters applies best to the analysis of circuit board assemblies remains to be determined by detailed validation studies.
- Model parameters show variability depending on the range of stress, strain rates and temperature covered by a given dataset. If anything, the variability in model parameters suggests extreme caution in the selection of a constitutive model. Moreover, constitutive models themselves need be validated by independent data before they can be used with confidence in the thermo-mechanical analysis of electronic solder joints.

Last, discrepancies were noticed between model parameters for SAC shear and tensile creep. While parameters for SAC and Sn-3.5Ag alloys are rather similar, in general, the analysis of SAC tensile data leads to lower activation energy than that of SAC in shear. This is possibly related to the thickness of SAC joints and constraining effects of soldered surfaces in shear as opposed to the stress-free surfaces of tensile specimens. More detailed studies are warranted to elucidate the underlying physics behind these differences.

Acknowledgments

This paper was written in memory of the late Dr. Andreas Schubert and to honor his many valuable contributions to the field of solder mechanics and solder joint reliability. Dr. Schubert will be dearly missed by this author and the entire microelectronics reliability community.

References

- Atsumi, K., “Creep properties of Sn-Ag-Bi and Sn-Ag-Cu lead free solder alloys”, MS thesis abstract, 2000, Graduate School of Material Science and Engineering, Shibaura Institute of Technology, Japan (available at: http://www.mc.mat.shibaura-it.ac.jp/~master/online/online2000/299105/299105.html).
- Clech, J-P., “Review and analysis of lead-free solder material properties”, chapter to appear in IEEE/Wiley book on NEMI’s Lead-Free Project (http://www.nemi.org), 2003.
- Darveaux, R., Banerji, K., Mawer, A. and Dody, G., “Reliability of plastic ball grid array assemblies”, Chapter 13, Ball Grid Array Technology, ed. J. H. Lau, McGraw-Hill, 1995, pp. 379-442.
- Dušek, M. and Hunt, C., “Measurement of materials properties of lead-free solders for modelling requirements”, Proceedings (CD-ROM), SMTA International Conference, Chicago, IL, September 21-25, 2003.
- Dušek, M. and Hunt, C., “Do we know enough about lead free solders?”, Proceedings, IPC/JEDEC 4th International Conference on Lead Free Electronic Assemblies and Components, Frankfurt, Germany, October 21-22, 2003, pp. 458-460.
- Fouassier, O., Ph.D. thesis (2001), University of Bordeaux, France, “Brasure composite sans plomb: de la conception a la caractérisation” (Thesis Part III), Sept. 24, 2001 (.pdf file on the web), Development of Adaptative Solder Technology for Reliability and Environment Compatibility of Electronic Assemblies, Brite/EuRam III Project No. BE97-5109.
- Morris, J.W., Song, H.G. and Hua, F., “Creep properties of Sn-rich solder joints”, Proceedings (CD-ROM), IEEE 53rd Electronic Components and Technology Conference, New-Orleans, LA, May 27-30, 2003.
- Pang, J.H.L., Xiong, B. S., Neo, C.C., Zhang, X.R. and Low, T.H., “Bulk solder and solder joint properties for lead-free 95.5Sn-3.8Ag-0.7Cu solder alloy”, Proceedings (CD-ROM), IEEE 53rd Electronic Components and Technology Conference, New-Orleans, LA, May 27-30, 2003.
- Wiese, S., Schubert, A., Walter, H., Dudek, R., Feustel, F., Meusel, E. and Michel, B., “Constitutive behavior of lead-free solders vs. lead-containing solders - Experiments on bulk specimens and flip-chip joints”, Proceedings, 51st Electronic Components and Technology conference, Orlando, FL, 2001, pp. 890-902.
- Wu, C.M.L. and Huang, M.L., “Creep behavior of eutectic Sn-Cu lead-free solder alloy”, Journal of Electronic Materials, Vol. 31, No. 5, 2002, pp. 442-448.
- Zhang, Q., Dasgupta, A. and Haswell, P., “Viscoplastic constitutive properties and energy-partitioning model of lead-free Sn3.9Ag0.6Cu solder alloy”, Proceedings (CD-ROM), IEEE 53rd Electronic Components and Technology Conference, New-Orleans, LA, May 27-30, 2003.